Biophysical Chemistry 156 (2011) 13–23

Contents lists available at ScienceDirect

Biophysical Chemistry

journal homepage: http://www.elsevier.com/locate/biophyschem

Applications of pressure perturbation calorimetry in biophysical studies

Yong Zhai [a], Linus Okoro [a], Alan Cooper [b], Roland Winter [a,*]

[a] TU Dortmund University, Faculty of Chemistry - Biophysical Chemistry, Otto-Hahn Str. 6, D-44227 Dortmund, Germany
[b] School of Chemistry, College of Science and Engineering, University of Glasgow, Glasgow G12 8QQ, UK

ARTICLE INFO

Article history:
Received 15 December 2010
Received in revised form 29 December 2010
Accepted 29 December 2010
Available online 4 January 2011

Keywords:
Pressure perturbation calorimetry
Protein folding
Ligand binding
Solvation
Cosolvents
α-lactalbumin
Phospholipids
Lipid phase transitions
Gramicidin
Cyclodextrin

ABSTRACT

Pressure perturbation calorimetry (PPC) is a relatively new and efficient technique, to study the volumetric properties of biomolecules in solution. In PPC, the coefficient of thermal expansion of the partial volume of the biomolecule is deduced from the heat consumed or produced after small isothermal pressure jumps (typically ± 5 bar). This strongly depends on the interaction of the biomolecule with the solvent or cosolvent as well as on its packing and internal dynamic properties. This technique, complemented by ultrasound velocity and densitometry, provides valuable insight into the basic thermodynamic properties of solvation and volume effects accompanying phase transitions and interactions of biomolecular systems. Here we review data on protein folding, ligand binding processes, and phospholipid phase transitions, together with discussion of interpretation and further significant applications.

Contents

1. Introduction . . . 13
2. PPC and related techniques . . . 14
2.1. PPC methodology . . . 14
2.2. Ultrasound velocity and densitometric measurements . . . 15
3. Observations and interpretations . . . 15
3.1. PPC measurements of proteins in various thermodynamic states . . . 16
3.2. Protein–ligand interactions. . . . 17
3.3. PPC studies of model biomembrane systems . . . 19
4. Concluding remarks . . . 22
Acknowledgement . . . 22
References . . . 22

1. Introduction

Pressure perturbation calorimetry (PPC) is a novel type of calorimetric technique that has become available in recent years in a form suitable for studying dilute samples in solution [1]. This calorimeter has basically the same architecture as a power-compensation differential scanning calorimeter (DSC), but measures the heat flow into or out of a sample upon small isothermal pressure changes. The method can be applied to study the thermal expansion coefficient (α) and relative volume changes of aqueous solutions and dispersions of chemical and biochemical systems, including amino acids, proteins, DNA and phospholipid vesicles, micellar systems, and polymers [1–16].

In general, the conformational stability of complex biomolecules such as proteins depends on temperature, pressure, hydration capacity and on the solvent properties. An important factor contributing to macromolecular stability is also the relative affinity towards a particular reagent (e.g., a cosolvent) in comparison to water or buffer solution. The influence of the protein surface on adjacent water and how this might be reflected in the apparent expansivity data of the protein has been discussed extensively by Lin et al. [1]. Their results indicate that exposed hydrophilic groups, such as charged or polar side chains of proteins, show a pattern

* Corresponding author.
E-mail address: roland.winter@tu-dortmund.de (R. Winter).

0301-4622/$ – see front matter © 2011 Elsevier B.V. All rights reserved.
doi:10.1016/j.bpc.2010.12.010

characteristic of water structure breakers, with a positive apparent expansion coefficient of the protein, in particular at low temperature, which decreases drastically with increasing temperature. On the contrary, apolar, hydrophobic amino acid side groups act in the reverse manner, as structure makers, by enhancing the space-consuming hydrogen-bonded network structure of water. Increasing thermal energy, however, may allow the water molecules to be released from the low-entropy denser layered structure or from the latter expanded less dense ordered solvation states. An example of such an effect is the gradual breakdown of low-density, ice-like clusters of water between 0 and 4 °C, a process that has a negative value of α. Hence, in general, for proteins in aqueous solution, the temperature dependent thermal expansion coefficient is potentially significantly influenced by protein–water interactions and therefore also by the magnitude of the solvent accessible surface area (SASA) of the protein. Moreover, irrespective of whether cosolvents directly interact with or are repelled by the protein, they are expected to induce changes in the quantity of hydration water and its associated properties, with consequences that will be reflected in the PPC data.

Complementary to densimetric measurements, the PPC technique has the very high sensitivity necessary to detect the small volumetric changes anticipated here. In fact, the relative volume changes of biomolecular systems, which can be either positive or negative, are usually very small (typically $\Delta V/V < 1\%$; for comparison, freezing of water causes a relative volume increase of 9%) [17–22]. Although densimetry has the advantage of providing absolute values of partial or apparent volumes, its precision in yielding expansitivies, and in particular expansivity peaks, accompanying phase and structural transitions is limited compared to PPC.

Because changes in solvation and packing also play a central role in the thermodynamics of non-covalent interactions in aqueous solution, PPC has also proved valuable in studying biomolecular interactions in solution, which are generally accompanied by changes in volumetric (packing) and solvation properties. This has recently been applied to the determination of expansibility changes associated with a range of non-covalent binding processes in solution, including protein–protein and protein–ligand interactions, together with comparable measurements on more rigid cyclodextrin host–guest complexes [23–27].

Here, after outlining the principle of the technique, we describe how PPC can be used to obtain volumetric properties of proteins in different conformational states, as well as upon ligand binding. In addition, we show how PPC can be used to study volumetric properties of model biomembrane systems undergoing phase transformations. Moreover, the use of combining PPC data with densitometric and ultrasound velocity data for yielding complementary thermodynamic information is discussed. Finally, we will discuss the complexities and ambiguities in interpretation of PPC and related data.

2. PPC and related techniques

2.1. PPC methodology

Pressure perturbation calorimetry measurements are typically carried out on the MicroCal (GE Healthcare) VP-DSC calorimeter equipped with the PPC accessory—see Fig. 1. This allows measurement of heat effects induced by small periodic changes of gas pressure ($\Delta p = \pm 5$ bar) applied equally to the sample and reference solutions. Multiple pressure-jumps in both directions are normally carried out automatically at a series of specified temperatures. The measurable is ΔQ—the heat released upon a pressure change of Δp at temperature T—which arises from differences in the heat generated reversibly from differences in the pressure × volume work on the sample and reference during compression or relaxation. This is related to the expansibility as follows.

Thermodynamics relates the pressure coefficient of the heat reversibly exchanged, $(\partial Q_{rev}/\partial p)_T$, to the coefficient of thermal expansion, $\alpha = (1/V)(\partial V/\partial T)_p$, of the sample volume. For a sufficiently dilute solution containing m grams of solute and m_0 grams of solvent, the volume is given by $V = m_0 V_0 + mV^o$, where V_0 is the specific volume

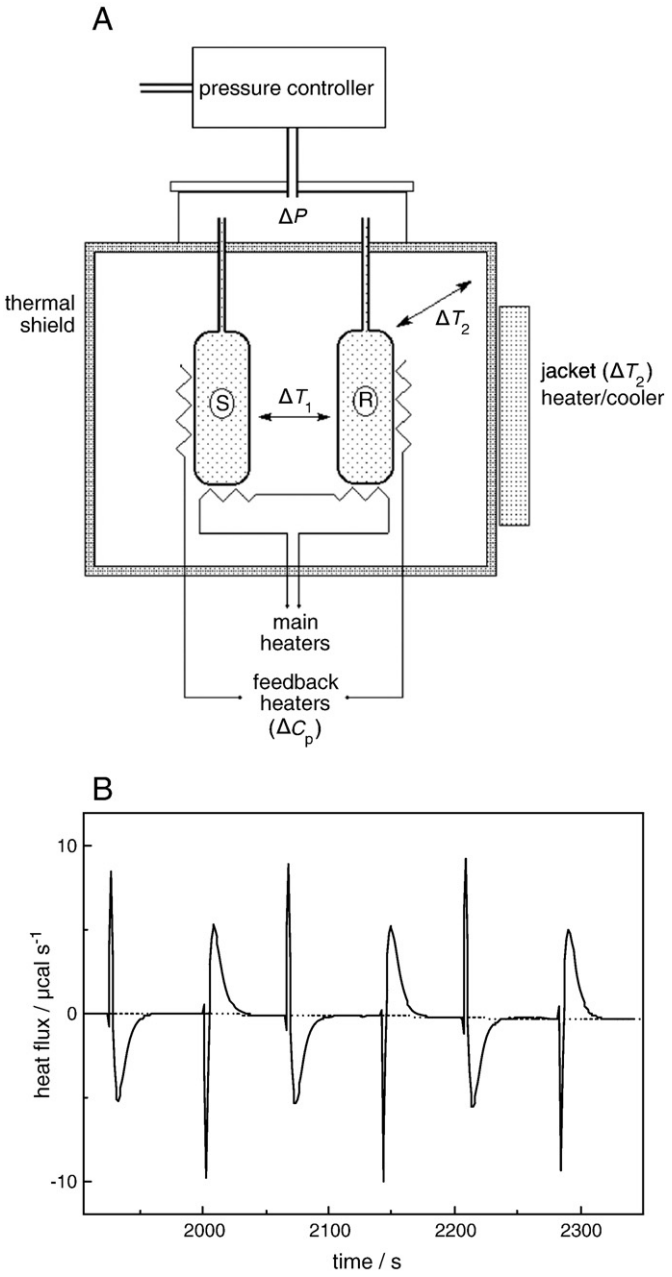

Fig. 1. (A) Diagram showing the basic principles of the PPC modification of the VP-DSC. (B) Example of raw PPC data showing the heat flux responses to consecutive pressure pulses (up/down) for a dilute aqueous protein solution at 25 °C.

of the solvent and V^o the partial specific volume of the solute. One then finds [1]:

$$(\partial Q_{rev}/\partial p)_T = -TV\alpha = -T\left[m_0 V_0 \alpha_0 + mV^o \alpha^o\right]. \quad (1)$$

where $\alpha_0 = (1/V_0)\ (\partial V_0/\partial T)_p$ and $\alpha = (1/V^\circ)(\partial V^\circ/\partial T)_p$ are the coefficients of thermal expansion associated with the solvent volume and the solute partial volume, respectively.

In the actual differential PPC experiment, with sample solution in the sample cell and buffer in the reference cell, both cells are subjected to the same pressure change, so that the net heat change will be equal to the difference between Eq. (1) for the sample cell and that for the reference cell. If the two cells have an identical volume, the heat change arises because the volume occupied by the solute in the sample cell, mV°, is replaced by the same volume of solvent in the reference cell, and

Eq. (1) can be integrated to yield the working equation

$$\Delta Q_{rev} = -T\left[mV^{\circ}\alpha^{\circ} - mV^{\circ}\alpha_0\right]\Delta p \tag{2}$$

which then rearranges to

$$\alpha^{\circ} = \alpha_0 - \frac{\Delta Q_{rev}}{TmV^{\circ}\Delta p}. \tag{3}$$

α_0 is determined in a separate PPC experiment, with buffer in the sample cell and pure water in the reference cell. For simplicity, in the remainder of this review, the value of the partial specific volume, V^o, and the coefficient of thermal expansion of the solute, α^o, will be replaced by their apparent values, denoted V and α, respectively.

The relative volume changes $\Delta V/V$ at the phase transitions of the biomolecular systems, taking place in the temperature interval from T_i to T_f (the onset and completion temperature of the peak, respectively) are obtained by:

$$\frac{\Delta V}{V} = \int_{T_i}^{T_f} \alpha(T)\mathrm{d}T. \tag{4}$$

From the relative volume changes $\Delta V/V$, the absolute specific volume changes ΔV can be determined using the relation $\Delta V = (\Delta V/V)/c$, where c is the concentration of the sample (given in mg mL^{-1}).

For the case of a two-state processes, Schweiker et al. [15,16] proposed a method of analyzing the data to determine the enthalpy and relative volume changes more accurately by simultaneous fitting both the DSC and PPC data.

2.2. Ultrasound velocity and densitometric measurements

Complementary techniques can be used to provide additional volumetric parameters that assist in evaluation and interpretation of PPC data [28,29]. The ultrasound velocity u in liquid samples may be determined using a differential ultrasonic resonator device (e.g. ResoScan, TF Instruments, Heidelberg, Germany) operating in a frequency range of 7.2 – 8.5 MHz [28,29]. The sound velocity in the sample is typically determined relative to that in the buffer solution at the same temperature in terms of the velocity number, $[u]$, defined as

$$[u] = (u - u_0)/u_0 c, \tag{5}$$

where u and u_o denote the sound velocities in the solution and in the solvent, respectively, and c is the solute concentration. The technique is applied to lipid solutions, here.

The densities, ρ and ρ_0, of the lipid solution and the solvent, respectively, can be measured using a high-precision density meter, the DMA 5000 (Anton Paar, Graz, Austria) for example, which is based on the mechanical oscillator principle. After correction for viscosity-induced errors, data may be used to evaluate the apparent specific volume of the sample, V, which, at low enough concentrations, approaches the partial specific volume, V^o.

The adiabatic compressibility coefficient, $\beta_S = -1/V\ (\partial V/\partial p)_S$, the speed of sound propagation, u, in the medium, and the density, ρ are related by the expression $\beta_S = (u^2\ \rho)^{-1}$. Slow relaxation processes, which appear, for example, around T_m of the gel-to-fluid lipid phase transition, may not be detected by β_S as measured by ultrasound velocity. The more meaningful thermodynamic parameter is the isothermal compressibility that can be obtained from the adiabatic compressibility when the thermal expansion and the heat capacity data are available. One obtains for of binary system of a solute in solvent ([28] and refs. therein):

$$k_T^o = k_S^o + \frac{T\alpha_0^2}{\rho_0 C_{p,0}}\left(2\frac{E^o}{\alpha_0} - \frac{C_p^o}{\rho_0 C_{p,0}}\right) \tag{6}$$

where k_T^o is the partial specific isothermal compressibility, k_S^o the partial specific adiabatic compressibility, α_0 and $C_{p,0}$ are the thermal expansion coefficient and the specific heat capacity of the solvent, respectively; $E^o = V^o\alpha^o$ and C_p^o are the partial specific expansivity and the partial specific heat capacity of the sample, respectively. The corresponding isothermal compressibility coefficient of the sample is obtained by $\beta_T = k_T^o/V^o$. Also in this case, apparent instead of partial specific quantities have been assumed, since the differences are expected to be rather small at the low concentrations normally used in these experiments.

The square average of the volume fluctuations $\langle \Delta V^2 \rangle$ of the solute is related to the isothermal compressibility data. Assuming that the partial specific volume is largely determined by the lipid itself, i.e. V^o reflects essentially the "real" volume of the lipid molecule, the relative volume fluctuations are given as [30–32]

$$\sqrt{\frac{\left\langle \Delta V^2 \right\rangle}{V^2}} = \sqrt{\frac{RT\beta_T}{MV^o}} \tag{7}$$

where M is the molar mass of the solute.

Following such procedures, it is usually possible to determine the sound velocity with a relative error smaller than 10^{-3}%, corresponding to a precision higher than 5×10^{-5} mL g^{-1} in $[u]$. Density values typically carry relative errors smaller than 10^{-3}%, so the accuracy in V^o is better than 10^{-4} mL g^{-1}. Therefore, considering the relative errors of $[u]$ and V^o, the uncertainty in k_S^o is within 10^{-12} mL g^{-1} Pa^{-1}.

3. Observations and interpretations

Earlier applications of PPC were directed towards establishing the effectiveness of the technique, focusing on volumetric properties of simple amino acids and peptides in solution, together with changes associated with simple thermal transitions in globular proteins and related systems. This work has been well covered elsewhere [1,4,16] and will not be revisited in detail here. Rather, we wish to concentrate on more recent observations involving a broader range of possibly more challenging systems, together with discussion of possible interpretations.

Before looking at more specific cases, it is worth mentioning some general considerations. As introduced by Chalikian et al. [19–21,33], changes in partial (or apparent) specific volume, and hence in the expansion coefficient α of a protein may be dissected into essentially three different contributions: 1) the intrinsic volume, V_{intr}, which originates from the van der Waals volume of the constituent atoms plus the volume of intrinsic voids within the water-inaccessible protein interior, 2) a hydrational term, δV_{hydr}, also denoted "interaction volume," describing–with regard to the bulk solvent–changes of the solvent volume associated with the hydration of solvent-accessible protein atomic groups, i.e., from solute–solvent interactions around the charged (electrostriction), polar (hydrogen-bonding), and nonpolar (hydrophobic hydration) atomic groups on the protein surface, and 3) the thermal volume, V_{therm}, which results from thermally induced mutual molecular vibrations and re-orientations of the solute and the solvent. The effect of the thermal volume is to expand the solvent away from the surface of the protein, such that solvent-free volume elements form around the protein. Altogether, one obtains: $V \approx V_{intr} + \delta V_{hydr} + V_{therm}$. The thermal expansivity of the protein interior is generally thought to be rather small [19–21], though this tentative conclusion may need to be re-evaluated as more data become available. The thermal volume is expected to increase with temperature, leading to a positive contribution to α. The solvation effect is also positive but, expected to decrease with increasing temperature as thermal activation leads to a continuous release of this low-entropy "condensed" water from the protein surface. Once the water is released, it no longer contributes to the partial volume of the protein and hence to α. Such a

behavior has indeed been found in recent experiments on amino acids and peptides, pointing to the fact that the hydrational term plays a major role in determining $\alpha(T)$ [8,9,34], at least for relatively small molecules with large surface-to-volume ratio. The negative volume change of unfolding observed for most proteins implies that at the transition temperature T_m, the opening of void volume and the increase in accessible surface area with more charged and polar groups upon unfolding overcompensate the positive effects of thermal volume and the decrease in the hydrophilic to hydrophobic balance of the SASA.

3.1. PPC measurements of proteins in various thermodynamic states

Recent work has investigated the solvation and volumetric properties of monomeric proteins such as ribonuclease A (RNase A) and staphylococcal nuclease (SNase), in their native and unfolded states. The effects of various chaotropic and kosmotropic cosolvents (e.g., glycerol, sucrose, urea, guanidinium hydrochloride (GdmCl),) on the solvation and unfolding behavior of the proteins were investigated [8,9,34,35]. The cosolvents not only markedly change the stability of proteins, but also their solvation, and they may also alter the conformation of the proteins in their unfolded, denatured states. The magnitude and even sign of the volume change of unfolding drastically depends on the cosolvent concentration. However, the volume change that accompanies the unfolding transition of a protein also depends markedly on the unfolding temperature, T_m. Addition of kosmotropic osmolytes (e.g., glycerol, sorbitol, sucrose) stabilizes the folded state, such that the T_m increases with increasing osmolyte concentration, and the relative volume change upon unfolding of RNase A, $d(\Delta V/V)/dT$, decreases roughly at a rate of $5\times10^{-4}\,K^{-1}$. Since the volume change of unfolding decreases with increasing temperature, we may conclude that at least part of the observed effect of the stabilizing cosolvents on ΔV is due to the increase in temperature (leading to an increase of V_{therm}) and not solely due to differential conformational effects. Such an explanation should also hold for the observed slight increase in the absolute value of ΔV as a function of increasing urea or GdmCl concentration ($d(\Delta V/V)/dT\approx4.7\times10^{-5}\,K^{-1}$ for RNase A), as these cosolvents destabilize the folded state of the protein leading to a decrease in the T_m with increasing denaturant concentration. The differences in $d(\Delta V/V)/dT$ values observed for the different cosolvent types implies, however, that the different ΔV values observed for the various types of cosolvents can only partially be explained by the temperature dependence of ΔV. An additional contribution must be due to differences in the structure of the unfolded state ensemble.

It is worth mentioning in passing that PPC has also been used recently to determine the volume and expansivity change of the temperature-induced helix-coil transition of polynucleotides, such as poly[$d(A-T)$] [14,36]. The transition, which depends on the ionic strength, is accompanied by a negative volume change and an increase in expansion coefficient. Similar to the case of protein unfolding, these results are consistent with a substantial increase of hydration in the unfolded coil form.

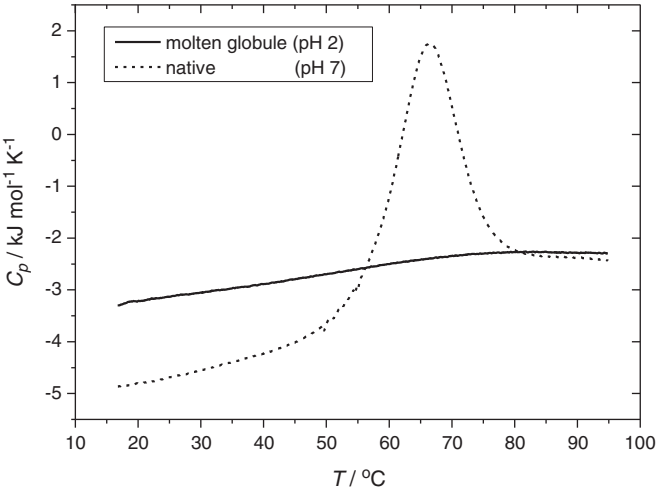

Fig. 2. DSC data of native BLA (at pH 7) and of the acidic-induced molten globule state of BLA (at pH 2) in the presence of 2 mM Ca^{2+}.

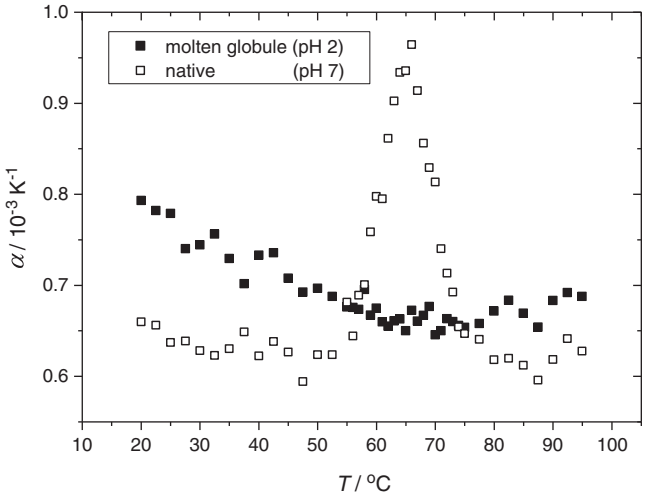

Fig. 3. PPC data of the native (at pH 7, open squares) and the acidic molten globule state (at pH 2, filled squares) of BLA in the presence of 2 mM Ca^{2+}.

Returning to proteins, here we would like to further address the use of the PPC method in characterizing volumetric properties of proteins in various conformational states, including the molten globule class of structures. Besides the compact native state and the denatured unfolded state, proteins can often adopt a rather compact denatured state that is generally referred to as "molten globule." The characteristics of a molten globule are: i) largely preserved native-like secondary structure, ii) partially disrupted tertiary structure, and iii) a compact structure with moderately increased radius of gyration [37].

α-Lactalbumin, a small Ca^{2+}-binding protein with 14.2 kDa molecular mass, is one of the most extensively studied and best characterized proteins and exhibits a stable molten globule state at low pH (e.g., at pH 2), at intermediate denaturant (urea, guanidinium hydrochloride) concentrations or in its calcium depleted form upon moderate heating [37]. DSC and PPC measurements have been carried out on native bovine α-lactalbumin (BLA) at pH 7 and on BLA in its molten globule state at pH 2. As shown in Figs. 2 and 3 no significant heat absorption or volume change is detected in the DSC or PPC measurements, respectively, for the acid-induced molten globule form at pH 2 as a function of temperature. Conversely, the native BLA at pH 7 shows an endothermic unfolding transition peak at 66 °C. The absence of pronounced calorimetric differences of the molten globule suggests that similar thermodynamic properties are shared by the thermally unfolded and the acidic molten globule state at high temperatures. The CD spectral ellipticity of the molten globule state at around 220 nm decreases monotonically with increasing temperature, even at high temperatures, indicating a gradual variation in the secondary structure only [38]. As depicted in Fig. 3, the expansion coefficient α of the molten globule is significantly larger than that of the natively folded protein, indicating a stronger hydration and possibly also larger void volume in the molten globule state. This would also be in agreement with the observation of an increased hydrophobic surface in the acidic-induced molten globule state as revealed by fluorescence spectroscopic and methylene radioactive labeling experiments [39–41]. Also the compressibility study by Kharakoz et al. [42] suggests that, in the molten globule state, the water molecules penetrate into the protein interior and interact with previously buried atomic groups, thus resulting in an increase in solvent accessible surface and enlarged hydration. It is also clearly seen that $\alpha(T)$ displays a slightly stronger

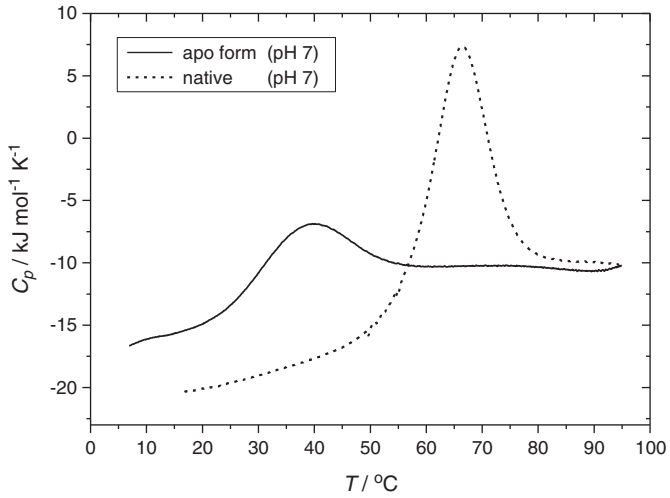

Fig. 4. DSC measurements of the calcium bound and calcium depleted form of BLA.

temperature dependence than the native protein at low temperatures (20–40 °C): $(d\alpha/dT)_{20-40} = -3.8\times10^{-6}$ K^{-2} for the molten globule and $(d\alpha/dT)_{20-40} = -1.4\times10^{-6}$ K^{-2} for the native protein.

A positive change in specific volume ΔV of 0.4% is observed in the PPC measurement of native α-lactalbumin upon thermal unfolding at $T = 66$ °C. At first glance, this result seems incompatible with most observations of negative volume changes accompanying protein unfolding. The relatively large positive volume increase for native α-lactalbumin implies an unusual unfolding pattern, however. FTIR and CD studies [43–45] of the thermal unfolding transition of α-lactalbumin revealed that, in the presence of calcium ions, the tertiary structure unfolds cooperatively during the thermal transition, while the secondary structure changes only gradually, resulting in a rather compact, partially unfolded structure with well conserved secondary structure [43–46], which shares almost similar characteristics with the acidic molten globule state.

Hence, the thermally unfolded state comprises a compact but expanded, lower density intrinsic structure with a relatively large void volume, and the expansion of its intrinsic volume compensates for the negative ΔV expected upon elimination of internal void typically observed for full unfolding of proteins at not too high temperatures. Besides the acidic-molten globule, the calcium depleted form (apo-form) of BLA reveals some interesting thermodynamic characteristics as well. DSC experiments show that the apo-form of BLA undergoes an unfolding transition at 37 °C, i.e. at a much lower temperature compared to the Ca^{2+} bound form of the protein, indicating marked destabilization of the protein by removal of Ca^{2+} ions (Fig. 4). Corresponding PPC measurements of the apo-form of BLA are depicted in Fig. 5. They reveal a positive volume change at the transition at this temperature as well. At such relatively low temperatures, proteins generally display negative volumes of unfolding. CD and proteolysis studies of BLA have shown that the apo-form of BLA exists as molten globule state [46,47], i.e. the transition can rather be described as native to molten globule kind of transition, which seems to be generally accompanied by positive volume changes. The volume increase is 0.24%, i.e. smaller than that of the calcium bound BLA. This would be in agreement with the general finding that the volume change of unfolding increases with increasing temperature, owing to the fact that the expansivity of the unfolded state is, to a first approximation, temperature independent, while that of the folded state decreases with increasing temperature [8].

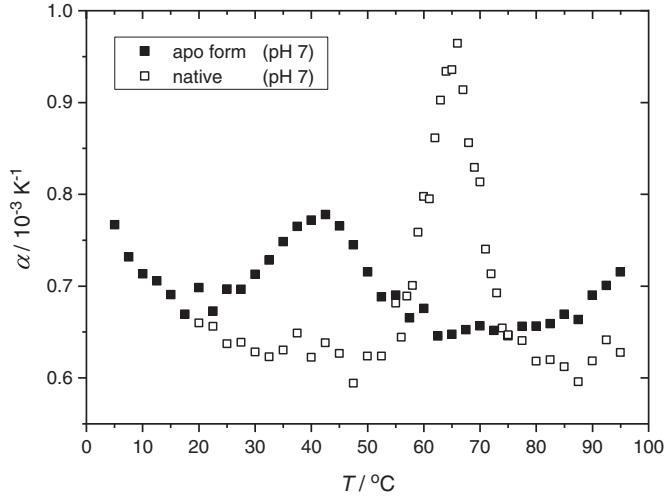

Fig. 5. PPC data of the calcium bound (open squares) and calcium depleted (filled squares) form of BLA. The calcium bound protein is measured in the presence of 2 mM Ca^{2+} and the calcium depleted upon addition of 2 mM EDTA.

In a recent study on SNase mutants it has been shown that at low temperatures the defining contribution to ΔV comes mainly from excluded volume differences and ΔV for unfolding is negative [8]. In contrast, at high temperatures, differential solvation due to the increased exposed surface area of the unfolded state and, in particular, its larger thermal volume linked to the increased conformational dynamics of the unfolded state ensemble takes over and ΔV for unfolding eventually becomes positive. As seen in this study [8], exceptions from such behavior are due to incomplete unfolding of the protein, such as upon formation of molten globule kind of structures that exhibit a higher flexibility and larger volume fluctuations, accompanied by a larger internal void volume and increased solvent accessible surface area.

One technical problem that can arise when estimating volume changes from PPC data is the difficulty in estimating an appropriate baseline for integration over the thermal transition region. However, a recent PPC study by Tsamaloukas et al. [48] has shown that, at least for fully unfolded proteins, the temperature dependence of the thermal expansion coefficient is well represented by a simple empirical polynomial expression. Moreover, the absolute value of $\alpha(T)$ for an unfolded protein is an additive function of the expansion coefficients of the individual amino acids. This seems physically reasonable for unfolded polypeptides, but is unlikely to be true for folded protein or other conformational states because of higher-order effects from void volumes and other features of more compact structures.

3.2. Protein–ligand interactions

Volumetric changes during ligand binding or other non-covalent protein interactions should yield potentially valuable information about solvation and other changes unrelated to major conformational change. In principle, one might anticipate that experimental data in such cases might be more readily interpreted, especially in examples where the structures of the proteins and their complexes are known, without the complexities arising from more extensive structural changes. However, as recent work has shown [26], even here the interpretation is not necessarily straightforward. Initial experiments [23,25] using PPC to explore volumetric changes upon binding of simple inhibitors at enzyme active sites, using both lysozyme: trisaccharide and ribonuclease:2'-CMP as representative models, showed significant changes in thermal expansivity upon complexation. Similar effects appeared in protein–protein binding experiments, using the pseudoazurin:cytochrome *c* peroxidase protein–protein interaction system [23,25]. In all cases, the thermal expansion coefficient (α) for the enzyme-inhibitor or protein–protein complex was found to be less than the sum of the thermal expansion coefficients for the separate components alone. The simplest explanation for this ubiquitous decrease in a range of protein interaction systems is that it arises predominantly from the reduction in total

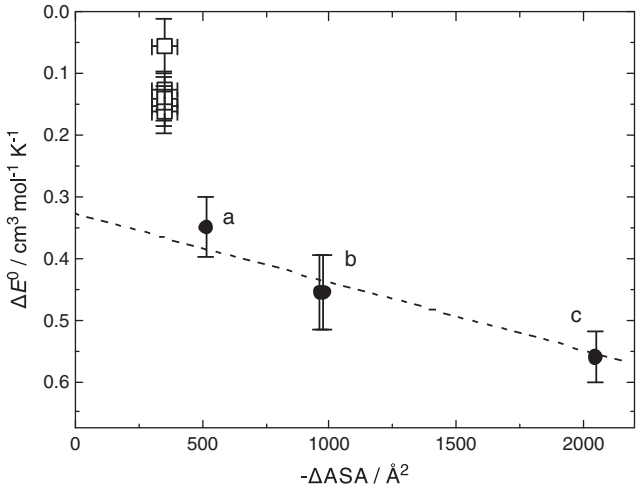

Fig. 6. Correlation of changes in molar expansivity (ΔE^{o}) with loss of solvent accessible surface area (ΔASA) upon binding. The dashed line is simply a guide to the eye, indicating approximate linear extrapolation of protein data. Open symbols (□) represent a range of cyclodextrin:adamantane host:guest complexes, whereas solid symbols (•) are for the protein–ligand (a: RNase:CMP, b: lysozyme:trisaccharide) and protein–protein (c: cytochrome:pseudoazurin) interactions. See [26] for details.

amounts of solvated water in the vicinity of the binding site and the ligand upon complex formation. The problem with this interpretation is that the (macro)molecules involved are inherently flexible structures, and it is not immediately possible to rule out volumetric changes related to ligand-induced effects on structural rigidity and packing densities within the protein–inhibitor complex [23]. Similar ambiguities arise in interpreting volumetric effects accompanying protein unfolding and other conformational transitions in biological macromolecules [19,20]. One route to clarification of the origins of thermal expansivity changes associated with non-covalent interactions in water has been described recently [26] using a combination of PPC, isothermal titration calorimetry (ITC) and standard volumetric (density) techniques applied to the cyclodextrin:adamantane host:guest system [24]. The advantage of this model system is that both the host (cyclodextrin) and the guests (adamantanes) are relatively rigid small molecules (compared to proteins), whose structures and interaction thermodynamics have been extensively studied [49]. This potentially allows comparison of thermodynamic binding parameters with associated volumetric and solvation changes in the absence of competing effects from conformation changes and dynamic modifications in the participating molecules.

As might be anticipated, the changes in thermal expansion coefficient and expansibility ($E^{\circ} = \partial V^{\circ}/\partial T = V^{\circ}\alpha$) upon complex formation are usually somewhat smaller than those found during major conformational transitions, so experiments can be quite challenging, but some interesting trends have emerged [26]. This is illustrated in Fig. 6, where changes in molar expansivity (ΔE^{o}) are compared with loss of solvent accessible surface area (ΔASA) upon binding for the various systems considered. Firstly, although the protein-based systems exhibit an apparently linear correlation between ΔE^{o} and ΔASA, the molar expansivity does not extrapolate to zero for the (hypothetical) case of ΔASA = 0. Secondly, expansibility changes are relatively much smaller for the much more rigid cyclodextrin:adamantane systems, and these do not follow the same trend as for protein binding. Both these observations indicate that, at least for protein binding interactions, loss of solvation (as expressed by decrease in solvent-accessible surface area) can explain only part of the loss of expansibility in these systems.

This is emphasized by estimates of the numbers of water molecules released (Δn_h) during binding. If one assumes that changes in expansibility are simply due to loss of hydration during binding, then $\Delta E^{o} = \Delta n_h(E_h - E_o)$, where E_h is the average molar expansivity of the n_h water molecules in the hydration shell, and E_o is the expansivity of water molecules in the bulk phase. Estimates for $(E_h - E_o)$ typically lie in the range 0.006–0.01 $cm^3\ mol^{-1}\ K^{-1}$, based on the volumetric properties of small molecules in water [50,51]. For the β-cyclodextrin complexes, using the PPC-derived ΔE^{o} data [26], this gives estimates of Δn_h of order 15–25 water molecules released upon adamantane binding. Such numbers are consistent with expectations from structural considerations and are in agreement with estimates obtained for similar complexes using volumetric and osmotic stress-related techniques [51,52]. Unfortunately, no such convenient comparison is found for the protein–ligand or protein–protein binding examples, where PPC-based estimates of Δn_h bear little relation to (equally questionable?) values obtained by other means.

Consequently, the overall conclusion from this reasonably comprehensive PPC study of binding in solution that solvation effects are only part of the story for protein interactions and that changes in macromolecular flexibility and dynamics may contribute extensively to binding thermodynamics and expansibility changes [26]. In particular, focusing on changes in solvent accessible surface area (ΔASA) alone might be misleading. Interestingly, a similar conclusion arises out of re-examination of heat capacity (ΔC_p) effects in protein systems [53]. In this context, it would perhaps not be surprising to see some degree of correlation between ΔC_p and ΔE^{o}, since both quantities reflect the temperature dependence of extensive thermodynamic properties (enthalpy, H, in the case of ΔC_p, molar volume, V°, for ΔE^{o}), and both depend–at least in part–on thermal excitation of interatomic motions (bear in mind that thermal expansion arises from heat-induced increases in interatomic or

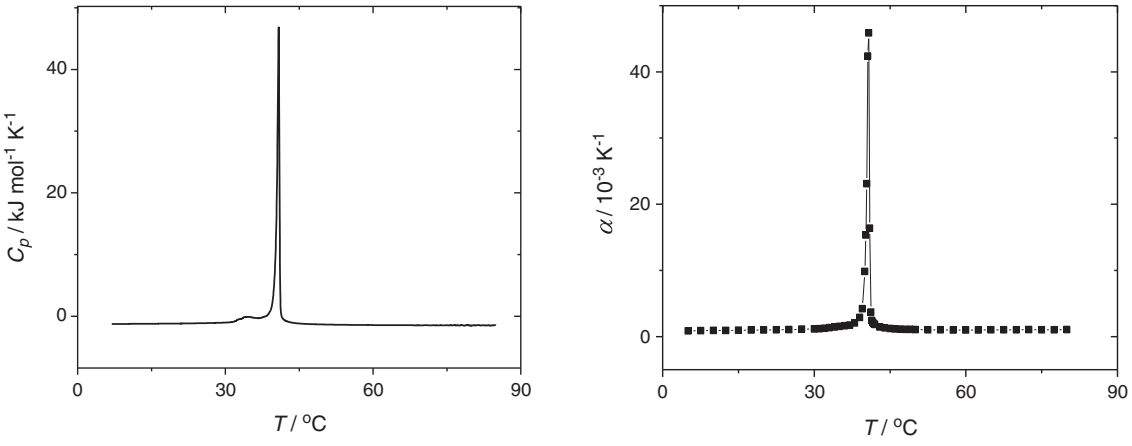

Fig. 7. DSC data (on the left) and PPC data (on the right) of aqueous dispersions of DPPC large unilamellar vesicles.

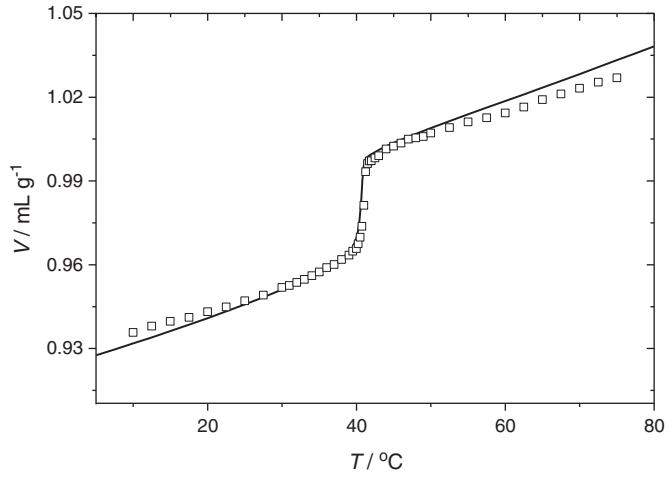

Fig. 8. Apparent specific volume V of DPPC vesicles from densitometry (□) and PPC data (—).

intermolecular distances as a result of thermal excitation of anharmonic molecular motions (dynamic effects) as well as from thermal redistribution of molecules or groups into different structural environments). It is to be expected, therefore, that such quantities might involve changes in dynamics dissipated throughout the macromolecule, and not simply confined to intermolecular surfaces.

3.3. PPC studies of model biomembrane systems

Studies of volumetric properties of lipid membranes supply important information about the intrinsic packing properties and hydration of the membrane. Densitometry and dilatometry have previously been used to determine the specific volume of lipids in solution [54–56]. However, measurements employing these techniques often meet practical limitations such as precise temperature control and high consumption of sample, so that PPC has turned out to be equally useful in studies of lipid mesophases and their phase transitions. As an example, the thermal expansion coefficient, α, of dispersions of 1,2-dipalmitoyl-*sn*-phosphatidylcholine (DPPC) is shown and compared to the corresponding DSC data in Fig. 7. Like the specific heat data, the expansion coefficient shows a similar sharp peak at the gel-to-fluid (main) transition temperature. The similarity in shape of the $C_p(T)$ and $\alpha(T)$ curves suggests a direct correlation between the enthalpy and volume changes at the phase transition. As shown below, they are also correlated with increasing amplitudes of volume fluctuations when approaching the phase transition temperature T_m [57].

Integration of the $\alpha(T)$ curve provides the relative volume change $\Delta V/V$ at the main transition, which is 3.2% for DPPC, in good agreement with the results based on previous densitometry and dilatometry data [54–56]. Using the $\alpha(T)$ values obtained from PPC, we can also calculate the partial specific volume of DPPC as a function of temperature. As seen in Fig. 8, reasonable agreement is obtained with the result obtained from direct densitometric measurements. Please note that the derivative of $V(T)$, i.e., the temperature dependence of the expansivity, can more accurately be obtained from PPC measurements.

Upon addition of various amounts of cholesterol to DPPC, and their mixtures with disordered phospholipids, different physico-chemical membrane properties can be obtained, including liquid-ordered (l_o) phases. Cholesterol causes a well known "condensing effect" in fluid membranes, and a liquid-ordered phase develops with increasing cholesterol concentration. PPC data on DPPC–cholesterol mixtures exhibit a drastic broadening of the main transition with increasing cholesterol content [28], corresponding to a continuous decrease of the volume change accompanying the phase transition, which is due to the increasing amount of liquid-ordered phase.

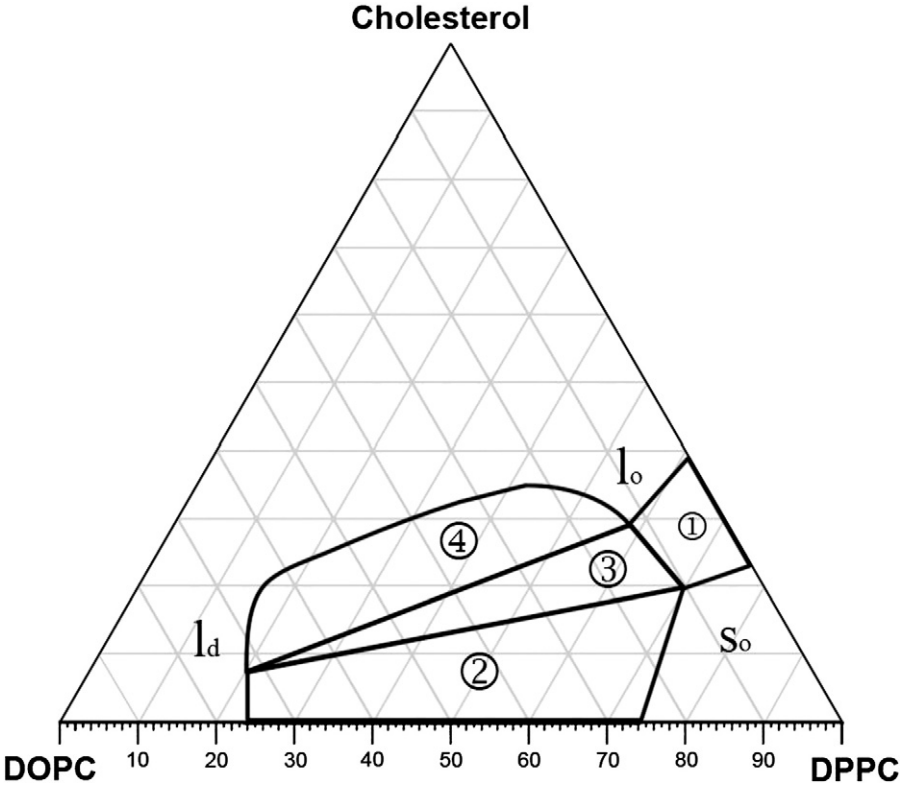

Fig. 9. Phase diagram of the ternary lipid mixture (DOPC/DPPC-d_{62}/Chol) at $T = 10$ °C. Different phase regions (s_o—gel phase, l_o—liquid-ordered phase, l_d—liquid-disorded phase, (1) $s_o + l_o$, (2) $s_o + l_d$, (3) $s_o + l_o + l_d$, (4) $l_o + l_d$) and phase boundaries are determined through ^{2}H-NMR spectroscopy (adopted from [58]).

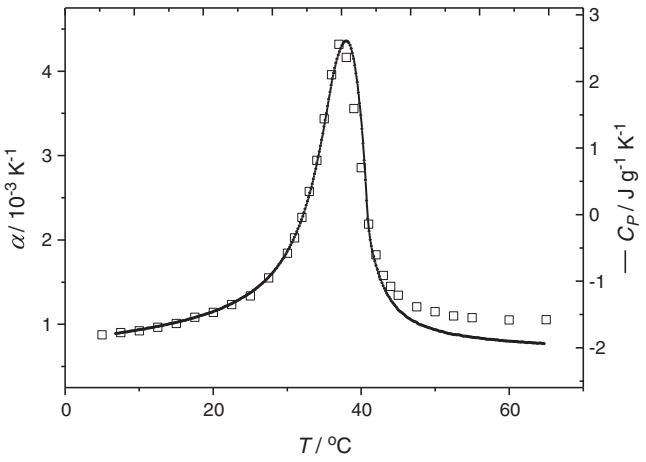

Fig. 10. DSC (—) and PPC (□) data of the ternary lipid mixture DOPC:DPPC 1:9 + 10% cholesterol (corresponding to DOPC:DPPC:Chol 9:81:10 molar ratio).

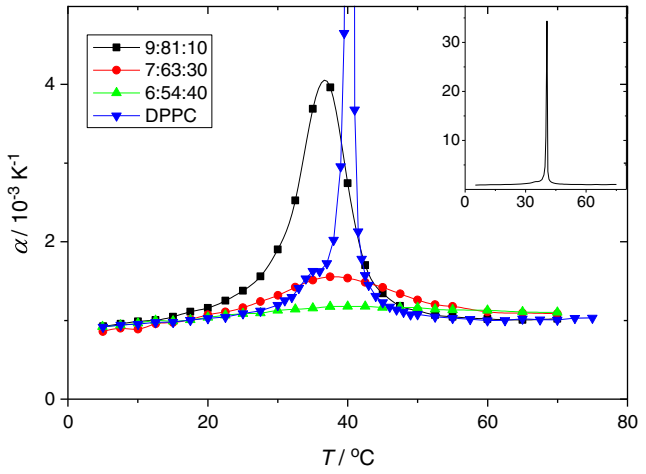

Fig. 11. PPC curves of ternary lipid mixtures with a lipid ratio DOPC:DPPC of 1:9 and different amounts of cholesterol.

Coexistence of liquid-ordered and liquid-disordered phases has been found for ternary lipid mixtures, such as for DOPC/DPPC/cholesterol mixtures at particular concentrations of their lipid constituents. This is illustrated in the phase diagram (Fig. 9) for deuterated DPPC at 10 °C. This was used in ^{2}H-NMR studies to determine the phase behavior of the system (please note that deuteration generally lowers the phase transition temperatures by a few degrees) [58]. The Gibbs phase triangle shown in Fig. 9 depicts the various lipid phases, representing single and coexisting phase regions and their corresponding lipid compositions.

PPC measurements have been carried out in order to explore the usefulness of this methodology in determining minor differences in the volumetric data of these different lipid mixtures. As illustrated in Fig. 10, the DSC and PPC peaks of ternary mixtures share the same shape at the corresponding phase transitions, indicating highly correlated enthalpy and volume changes. Fig. 11 shows PPC data of the DOPC:DPPC 1:9 mixture for different cholesterol concentrations. Since the lipid mixtures measured refer to different phase regions, the lipid samples undergo different types of phase transitions with increasing temperature. The absolute α-values do not furnish unambiguous evidence for distinguishing different phases as the differences in α-values are very small. On the other hand, however, the volume changes accompanying the phase transitions are quite distinct. The lipid mixture DOPC:DPPC = 1:9 + 10% Chol (i.e. DOPC:DPPC:Chol 9:81:10 molar ratio) undergoing the gel (solid-ordered, s_o) to fluid (l_d phase) phase transition ($s_o \rightarrow l_d$) transition exhibits the largest $\Delta V/V$ value of 2.8%, which is thus comparable to the chain melting transition of pure DPPC dispersions. Upon increasing the cholesterol or DOPC content, the volume change decreases. A sample (DOPC:DPPC = 1:9 + 30% Chol) undergoing the $s_o + l_o \rightarrow l_d$ transition exhibits a relative volume change of 1.0%. As might be expected, the temperature-induced fluid-fluid $l_o \rightarrow l_d$ transition (as observed for the DOPC:DPPC = 1:9 + 40% Chol mixture) can hardly be detected anymore (the relative volume change can still be estimated to be ~0.3%). The $l_o + l_d \rightarrow l_d$ miscibility transition of the sample DOPC:DPPC = 1:2 + 30% Chol exhibits a $\Delta V/V$ value of 0.8%, and that for the $s_o \rightarrow l_d$ transition (DOPC:DPPC = 1:1 + 0% Chol—data not shown) a relative volume change of 1.5%.

As shown by these data, cholesterol incorporation in the lipid mixtures has a strong potential for reducing the volume change accompanying the phase transitions. The rationale is as follows: on one hand, the cholesterol molecule perturbs the organization and packing of the ordered gel phase and increases the partial volume of membrane lipids; on the other hand, it increases the order parameter of the liquid-disordered phase and reduces the corresponding partial lipid volume in this phase. The counteracting disordering and ordering effects cause the drastically reduced volume change observed for the constant DOPC:DPPC ratio upon increasing the cholesterol contents (Fig. 11).

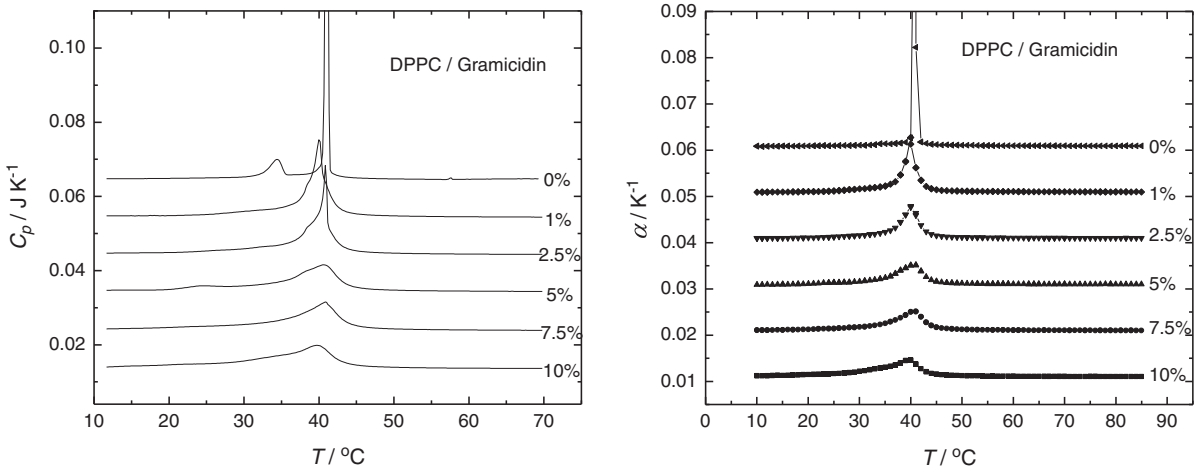

Fig. 12. –Left: DSC thermograms of pure DPPC and DPPC-gramicidin mixtures in excess water (expanded view also for pure DPPC). Right: Temperature dependence of the coefficient of thermal expansion, α, of pure DPPC and DPPC-gramicidin mixtures (pH 7.4). To facilitate better visibility, the curves are displaced along the y-axis (from bottom to top by 0.01 units).

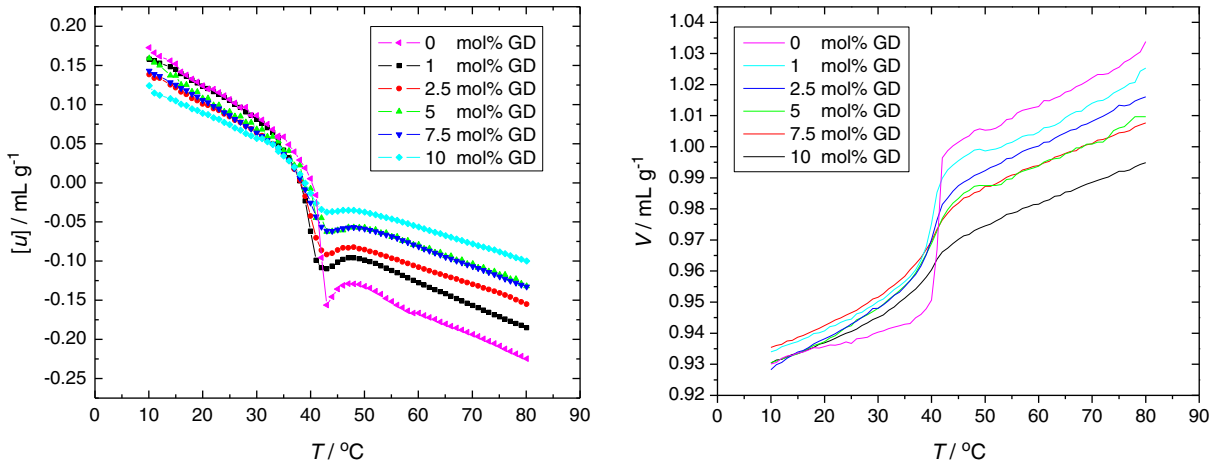

Fig. 13. The temperature dependence of the ultrasound velocity number [u] (left) and the apparent specific volume V (right) of DPPC-gramicidin mixtures.

Finally, these data also show that PPC is in fact able to determine minute volume changes in complex lipid mixtures.

As a last example, we discuss the effect of peptide insertion into phospholipid bilayers on the volumetric properties of the system. Gramicidin D (GD) was incorporated into DPPC bilayers at mole fractions of up to 10%. The apparent specific volume, the relative volume changes, and the thermal expansion coefficients of the lipid-GD mixtures were determined using PPC and densitometry, together with complementary bilayer membrane compressibility data by molecular acoustics (ultrasound velocimetry, densitometry) measurements. The membrane compressibility is also closely related to the lipid chain ordering and to changes in the lipid bilayer hydration.

One of the first known antibiotics, gramicidin, belongs to a family of linear pentadecapeptide compounds produced by *Bacillus brevis*, a soil bacterium. Gramicidins are composed of alternating D- and L-amino acids and form β-type helices with a hydrogen-bonding pattern of the backbone similar to that in β-sheets. The primary interest of gramicidin lies in its ability to form ion channels in lipid membranes [59]. Gramicidin has no charged or hydrophilic chains, and its aqueous solubility is low. As both the amino and carboxy termini of the molecule are blocked, gramicidin has been found to partition strongly into the hydrophobic region of phospholipid membranes [59–65].

The DSC and PPC measurements were carried out at concentrations of 1, 2.5, 5, 7.5, and 10 mol% of gramicidin. Fig. 12 shows the DSC heat capacity traces (as stacked plot) of DPPC dispersions containing different concentrations of gramicidin. Pure DPPC displays the sharp main transition at $T_m = 41$ °C, as well as a small endothermic peak due to the $L_{\beta'}$–$P_{\beta'}$ pretransition, appearing at 35 °C. At concentrations of GD as low as 1%, we already observe significant broadening (with a small asymmetry at the low temperature end) of the main transition and a shift to a lower temperature. This behavior suggests that there is a higher peptide-lipid interfacial energy in the gel phase, so that intercalation of the peptide between gel and fluid domains lowers the overall line tension and thus the cooperativity, i.e., ΔH, of the melting transition [66]. At 2.5% and higher GD concentrations, the main peak position remains essentially unchanged, while the transition becomes more broadened. At 2.5% GD, a broad shoulder at the low-temperature side of the DSC peak is observed, which suggests appearance of an ordered-fluid two-phase region. Since the fluid lipids are shorter than the gel lipids, one may expect a better matching of the fluid lipids with GD, and therefore a shift of the C_p-profile to lower temperatures.

Fig. 12 reveals the corresponding PPC data as well. Again, the PPC peaks exhibit the same shape as the DSC traces, indicating that the membrane enthalpy and volume changes share a common origin (probably packing and hydration effects). Generally, C_p and α are directly related to fluctuation parameters. The square average of the enthalpy fluctuations, $\langle \Delta H^2 \rangle$, is determined by the heat capacity, C_p, of the system, and the covariance between H and V fluctuations, $\langle \Delta H\, \Delta V \rangle$, is related to the thermal expansion coefficient [30–32]: $\langle \Delta H^2 \rangle = RT^2 C_p$, and $\langle \Delta H \Delta V \rangle = RT^2 V\alpha$. Below the main transition temperature of DPPC, α increases nearly linearly with temperature. Around the phase transition temperature, α undergoes a sharp increase, reaches a maximum of about 0.12 K^{-1} at T_m (41 °C), and then rapidly decreases with increasing temperature, to reach a value nearly equal to that obtained below the transition temperature (α is ~0.93×10^{-3} K^{-1} below the pretransition (20 °C) and ~1.0×10^{-3} K^{-1} above the main transition (65 °C)). The observed α-value of pure DPPC is similar to the thermal expansivity of pure liquid hydrocarbons, such as tetradecane ($\alpha = 0.9\times10^{-3}$ K^{-1}), but an order of magnitude larger than that of bulk water ([28] and refs. therein). A slight increase in α below the pretransition is observed with increasing gramicidin concentration. For example, $\alpha = 1.12\times10^{-3}$ K^{-1} for 5 mol%, and $\alpha = 1.25\times10^{-3}$ K^{-1} for 7.5 mol% GD at 20 °C, while in the fluid phase at 65 °C, no significant change in α is detected.

The relative volume changes, $\Delta V/V$ are obtained by integration over the PPC peaks (Eq. 4). $\Delta V/V = 0.04 \pm 0.007$ (4%), corresponding to an absolute volume change of 29 mL mol^{-1} for pure DPPC; $\Delta V/V$ is 0.028 ± 0.001 for 1 mol%, 0.026 ± 0.002 for 2.5 mol%, 0.023 ± 0.002 for 5 mol% GD, and continues to decrease with further increasing

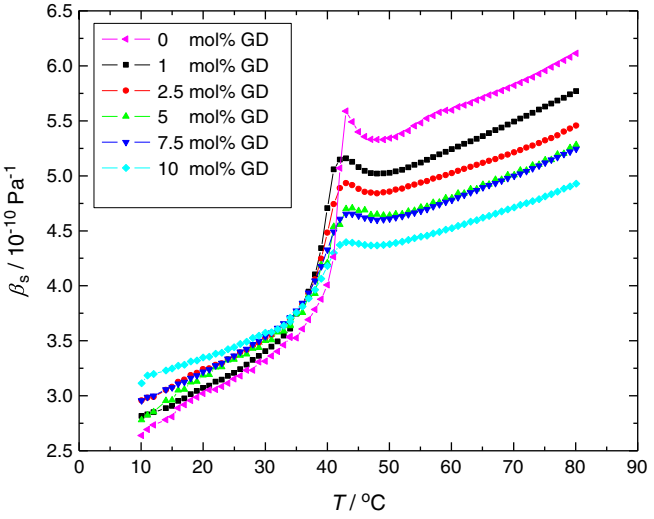

Fig. 14. Temperature dependence of the adiabatic compressibility coefficient, β_S, of DPPC large unilamellar vesicle dispersions and DPPC–gramicidin mixtures at different gramicidin molar fractions.

gramicidin concentration, finally reaching $\Delta V/V = 0.013 \pm 0.002$ at 10 mol% GD.

Ultrasound velocimetry and densitometry techniques have been used to measure the velocity number, $[u]$, and the apparent specific volume V of the DPPC-gramicidin mixtures as well (Fig. 13). At points distant from the lipid main phase transition temperature, T_m, $[u]$ decreases gradually with rise in temperature, finally leading to the typical anomalous dip in the vicinity of T_m typical for pure phospholipid bilayers [28,67–69]. Addition of gramicidin leads to a broadening of the peak around T_m and a slight shift towards lower temperatures. Compared to pure DPPC dispersions, $[u]$ is smaller below T_m and larger above T_m. The temperature dependence of the apparent specific volume is also shown in Fig. 14. An increase of V with temperature is observed throughout the whole melting transition regime. For pure DPPC, a step-like 4% change in specific volume at the transition temperature T_m is observed. For the DPPC–GD mixtures, the specific volume is larger below T_m and smaller above T_m. The adiabatic compressibility data derived from both data sets are shown in Fig. 14.

Finally, from the combined ultrasound, densitometric and PPC data, the isothermal compressibility and hence relative volume fluctuations (which are related to spontaneous pore formation and the permeability of the membrane) can be determined (Eq. 7). The isothermal compressibility peak at the main transition drops drastically (~75%) upon addition of GD concentrations as low as 1 mol% (data not shown). This decrease in β_T corresponds to a similar strong decrease (80%) of the thermal expansion coefficient (Fig. 12), again indicating the close relationship between the corresponding fluctuations ($\langle \Delta V^2 \rangle$ and $\langle \Delta H \Delta V \rangle$, respectively. At GD concentrations higher than 5 mol%, β_T is greater than β_S in the gel–fluid region by ~ 10–20%. The relative volume fluctuations are depicted in Fig. 15. They reach their maximum value of 12% for DPPC at the main transition, and are already strongly damped at a GD concentration of 1 mol%. Only a gradual further decrease with GD concentration is observed between concentrations of 1 and 10 mol%.

4. Concluding remarks

PPC is not an easy technique to apply, and analysis and interpretation of resulting data can still pose problems. At the experimental level, sensitivity is often limited by the large thermal transients or oscillations induced by the pressure pulses (see Fig. 1 for example). The origin of these transients is not clear, but an appropriate choice of baseline for integration can be difficult in this region. Moreover, the pressure-induced heat effects are usually quite small, such that current instruments require relatively high concentrations of biomolecules, and this can limit applicability. There also remain difficulties in unambiguously separating solvation from conformational dynamics or other volumetric effects.

Generally, however, the examples shown above demonstrate that the PPC technique has the potential to provide an exquisitely sensitive handle on measurements of volumetric and hydration properties of biomolecules such as lipids and proteins, the understanding of which is prerequisite to the comprehension of their stability and conformational dynamics. The PPC results on proteins in various chaotropic and kosmotropic cosolvents show that the cosolvent not only markedly changes the stability of proteins, but also its solvation, and it may also alter the conformation of the protein in its unfolded, denatured state. The magnitude and even sign of the volume change of unfolding drastically depends on the cosolvent concentration, but is also markedly temperature dependent. Moreover, conformational changes of the protein are clearly reflected in their volumetric properties and can thus be uncovered by PPC measurements. We have come to understand, at least qualitatively, the underlying molecular contributions to the volumetric properties of the various states of proteins and how these change with temperature. These results underscore the complexity of volumetric properties of biomolecules and demonstrate that their interpretation in terms of solvation coupled with conformational transitions should be interpreted in the context of their complete temperature dependence. What is also clear, however, is that further efforts are needed to establish quantitative models for interpretation of PPC data.

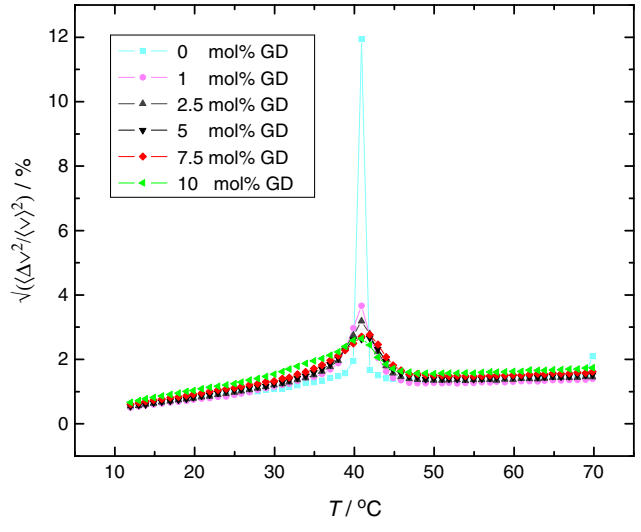

Fig. 15. Temperature dependence of the relative volume fluctuations of DPPC–GD mixtures at different GD molar fractions.

Acknowledgement

Financial support from the BMBF, the country Northrhine Westfalia, the European Union (Europäischer Fonds für regionale Entwicklung) and the BBSRC (UK) is gratefully acknowledged.

References

[1] L.N. Lin, J.F. Brandts, J.M. Brandts, V. Plotnikov, Determination of the volumetric properties of proteins and other solutes using pressure perturbation calorimetry, Anal. Biochem. 302 (2002) 144–160.
[2] P.L.G. Chong, R. Ravindra, M. Khurana, V. English, R. Winter, Pressure perturbation and differential scanning calorimetric studies of bipolar tetraether liposomes derived from the thermoacidophilic archaeon *Sulfolobus acidocaldarius*, Biophys. J. 89 (2005) 1841–1849.
[3] H. Heerklotz, Triton promotes domain formation in lipid raft mixtures, Biophys. J. 83 (2002) 2693–2701.
[4] H. Heerklotz, Pressure perturbation calorimetry, in: H.M. Dopico (Ed.), Methods in Molecular Biology, Springer, Berlin, 2007, pp. 197–206.
[5] H. Heerklotz, J. Seelig, Application of pressure perturbation calorimetry to lipid bilayers, Biophys. J. 82 (2002) 1445–1452.
[6] H. Heerklotz, A. Tsamaloukas, K. Kita-Tokarczyk, P. Strunz, T. Gutberlet, Structural, volumetric, and thermodynamic characterization of a micellar sphere-to-rod transition, J. Am. Chem. Soc. 126 (2004) 16544–16552.
[7] P. Kujawa, F.M. Winnik, Volumetric studies of aqueous polymer solutions using pressure perturbation calorimetry: a new look at the temperature-induced phase transition of poly(N-isopropylacrylamide) in water and D2O, Macromolecules 34 (2001) 4130–4135.
[8] L. Mitra, J.B. Rouget, B. Garcia-Moreno, C.A. Royer, R. Winter, Towards a quantitative understanding of protein hydration and volumetric properties, Chemphyschem 9 (2008) 2715–2721.
[9] L. Mitra, N. Smolin, R. Ravindra, C. Royer, R. Winter, Pressure perturbation calorimetric studies of the solvation properties and the thermal unfolding of proteins in solution—experiments and theoretical interpretation, Phys. Chem. Chem. Phys. 8 (2006) 1249–1265.
[10] C. Nicolini, J. Kraineva, M. Khurana, N. Periasamy, S.S. Funari, R. Winter, Temperature and pressure effects on structural and conformational properties of POPC/SM/cholesterol model raft mixtures—a FT-IR, SAXS, DSC, PPC and Laurdan fluorescence spectroscopy study, Biochim. Biophys. Acta, Biomembr. 1758 (2006) 248–258.
[11] L. Okoro, R. Winter, Pressure perturbation calorimetric studies on phospholipid-sterol mixtures, Z. Naturforsch., B: J. Chem. Sci. 63 (2008) 769–778.
[12] R. Ravindra, R. Winter, On the temperature—pressure free-energy landscape of proteins, Chemphyschem 4 (2003) 359–365.

[13] R. Ravindra, R. Winter, Pressure perturbation calorimetry: a new technique provides surprising results on the effects of co-solvents on protein solvation and unfolding behaviour, Chemphyschem 5 (2004) 566–571.
[14] G. Rayan, A.D. Tsamaloukas, R.B. Macgregor, H. Heerklotz, Helix-coil transition of DNA monitored by pressure perturbation calorimetry, J. Phys. Chem. B 113 (2009) 1738–1742.
[15] K.L. Schweiker, V.W. Fitz, G.I. Makhatadze, Universal convergence of the specific volume changes of globular proteins upon unfolding, Biochemistry 48 (2009) 10846–10851.
[16] K.L. Schweiker, G.I. Makhatadze, Use of pressure perturbation calorimetry to characterize the volumetric properties of proteins, in: methods in enzymology, Biothermodynamics 466 (Pt B) (2009) 527–547.
[17] H. Seemann, R. Winter, Volumetric properties, compressibilities and volume fluctuations in phospholipid–cholesterol bilayers, Zeitschr. fuer Phys. Chem. Int. J. Res. Phys. Chem. Chem. Phys. 217 (2003) 831–846.
[18] M. Bottner, D. Ceh, U. Jacobs, R. Winter, High-pressure volumetric measurements on phospholipid-bilayers, Zeitschr. Phys. Chem. 184 (1994) 205–218.
[19] T.V. Chalikian, Volumetric properties of proteins, Annu. Rev. Biophys. Biomol. Struct. 32 (2003) 207–235.
[20] T.V. Chalikian, K.J. Breslauer, On volume changes accompanying conformational transitions of biopolymers, Biopolymers 39 (1996) 619–626.
[21] T.V. Chalikian, R. Filfil, How large are the volume changes accompanying protein transitions and binding? Biophys. Chem. 104 (2003) 489–499.
[22] J. Rosgen, H.J. Hinz, Response functions of proteins, Biophys. Chem. 83 (2000) 61–71.
[23] A. Cooper, C.M. Johnson, J.H. Lakey, M. Nollmann, Heat does not come in different colours: entropy-enthalpy compensation, free energy windows, quantum confinement, pressure perturbation calorimetry, solvation and the multiple causes of heat capacity effects in biomolecular interactions, Biophys. Chem. 93 (2001) 215–230.
[24] D. Cameron, A. Cooper, Pressure perturbation calorimetry of solvation changes in cyclodextrin complexes, J. Incl. Phenom. Macrocycl. Chem. 44 (2002) 279–282.
[25] A. Cooper, D. Cameron, J. Jakus, G.W. Pettigrew, Pressure perturbation calorimetry, heat capacity and the role of water in protein stability and interactions, Biochem. Soc. Trans. 35 (2007) 1547–1550.
[26] D.L. Cameron, J. Jakus, S.R. Pauleta, G.W. Pettigrew, A. Cooper, Pressure perturbation calorimetry and the thermodynamics of noncovalent interactions in water: comparison of protein–protein, protein–ligand, and cyclodextrin–adamantane complexes, J. Phys. Chem. B 114 (2010) 16228–16235.
[27] A. Cooper, Microcalorimetry of heat capacity and volumetric changes in biomolecular interactions - the link to solvation? J. Therm. Anal. 104 (2011) 69–73.
[28] R. Krivanek, L. Okoro, R. Winter, Effect of cholesterol and ergosterol on the compressibility and volume fluctuations of phospholipid-sterol Bilayers in the critical point region: a molecular acoustic and calorimetric study, Biophys. J. 94 (2008) 3538–3548.
[29] V. Smirnovas, R. Winter, T. Funck, W. Dzwolak, Thermodynamic properties underlying the alpha-helix-to-beta-sheet transition, aggregation, and amyloidogenesis of polylysine as probed by calorimetry, densimetry, and ultrasound velocimetry, J. Phys. Chem. B 109 (2005) 19043–19045.
[30] A. Cooper, Thermodynamic fluctuations in protein molecules, Proc. Natl Acad. Sci. USA 73 (1976) 2740–2741.
[31] A. Cooper, Protein fluctuations and the thermodynamic uncertainty principle, Prog. Biophys. Mol. Biol. 44 (1984) 181–214.
[32] T.L. Hill, An Introduction to Statistical Thermodynamics, Dover, New York, 1960.
[33] T.V. Chalikian, Structural thermodynamics of hydration, J. Phys. Chem. B 105 (2001) 12566–12578.
[34] R. Ravindra, C. Royer, R. Winter, Pressure perturbation calorimetic studies of the solvation properties and the thermal unfolding of staphylococcal nuclease, Phys. Chem. Chem. Phys. 6 (2004) 1952–1961.
[35] J.D. Batchelor, A. Olteanu, A. Tripathy, G.J. Pielak, Impact of protein denaturants and stabilizers on water structure, J. Am. Chem. Soc. 126 (2004) 1958–1961.
[36] A.I. Dragan, D.J. Russell, P.L. Privalov, DNA hydration studied by pressure perturbation scanning microcalorimetry, Biopolymers 91 (2009) 95–101.
[37] K. Kuwajima, The molten globule state as a clue for understanding the folding and cooperativity of globular–protein structure, Proteins 6 (1989) 87–103.
[38] K. Kuwajima, Y. Hiraoka, M. Ikeguchi, S. Sugai, Comparison of the transient folding intermediates in lysozyme and alpha-lactalbumin, Biochemistry 24 (1985) 874–881.
[39] P.O. Craig, G.E. Gomez, D.B. Ureta, J.J. Caramelo, J.M. Delfino, Experimentally approaching the solvent-accessible surface area of a protein: insights into the acid molten globule of bovine alpha-lactalbumin, J. Mol. Biol. 394 (2009) 982–993.
[40] D.A. Kelkar, A. Chaudhuri, S. Haldar, A. Chattopadhyay, Exploring tryptophan dynamics in acid-induced molten globule state of bovine alpha-lactalbumin: a wavelength-selective fluorescence approach, Eur. Biophys. J. 39 (2010) 1453–1463.
[41] A.K. Lala, P. Kaul, Increased exposure of hydrophobic surface in molten globule state of alpha-lactalbumin-fluorescence and hydrophobic photolabeling studies, J. Biol. Chem. 267 (1992) 19914–19918.
[42] D.P. Kharakoz, V.E. Bychkova, Molten globule of human alpha-lactalbumin: hydration, density, and compressibility of the interior, Biochemistry 36 (1997) 1882–1890.
[43] D.A. Dolgikh, R.I. Gilmanshin, E.V. Brazhnikov, V.E. Bychkova, G.V. Semisotnov, S.Y. Venyaminov, O.B. Ptitsyn, Alpha-lactalbumin—compact state with fluctuating tertiary structure, FEBS Lett. 136 (1981) 311–315.
[44] W. Dzwolak, M. Kato, A. Shimizu, Y. Taniguchi, FTIR study on heat-induced and pressure-assisted cold-induced changes in structure of bovine alpha-lactalbumin: stabilizing role of calcium ion, Biopolymers 62 (2001) 29–39.
[45] G. Vanderheeren, I. Hanssens, Thermal unfolding of bovine alpha-lactalbumin—comparison of circular-dichroism with hydrophobicity measurements, J. Biol. Chem. 269 (1994) 7090–7094.
[46] D.A. Dolgikh, L.V. Abaturov, I.A. Bolotina, E.V. Brazhnikov, V.E. Bychkova, R.I. Gilmanshin, Y.O. Lebedev, G.V. Semisotnov, E.I. Tiktopulo, O.B. Ptitsyn, Compact state of a protein molecule with pronounced small-scale mobility—bovine alpha-lactalbumin, Eur. Biophys. J. 13 (1985) 109–121.
[47] P.P. de Laureto, E. Frare, R. Gottardo, A. Fontana, Molten globule of bovine alpha-lactalbumin at neutral pH induced by heat, trifluoroethanol, and oleic acid: a comparative analysis by circular dichroism spectroscopy and limited proteolysis, Proteins: Struct., Funct., Bioinf. 49 (2002) 385–397.
[48] A.D. Tsamaloukas, N.K. Pyzocha, G.I. Makhatadze, Pressure perturbation calorimetry of unfolded proteins, J. Phys. Chem. B 114 (2010) 16166–16170.
[49] M.V. Rekharsky, Y. Inoue, Complexation thermodynamics of cyclodextrins, Chem. Rev. 98 (1998) 1875–1917.
[50] C. Klofutar, J. Horvat, D. Rudan-Tasic, Apparent molar volume and apparent molar expansibility of sodium saccharin, potassium acesulfame and aspartame, Acta Chim. Slov. 53 (2006) 274–283.
[51] N. Taulier, T.V. Chalikian, Hydrophobic hydration in cyclodextrin complexation, J. Phys. Chem. B 110 (2006) 12222–12224.
[52] D. Harries, D.C. Rau, V.A. Parsegian, Solutes probe hydration in specific association of cyclodextrin and adamantane, J. Am. Chem. Soc. 127 (2005) 2184–2190.
[53] A. Cooper, Protein heat capacity: an anomaly that maybe never was, J. Phys. Chem. Lett. 1 (2010) 3298–3304.
[54] M. Boettner, R. Winter, Influence of the local-anesthetic tetracaine on the phase-behavior and the thermodynamic properties of phospholipid-bilayers, Biophys. J. 65 (1993) 2041–2046.
[55] D.L. Melchior, F.J. Scavitto, J.M. Steim, Dilatometry of dipalmitoyllecithin-cholesterol bilayers, Biochemistry 19 (1980) 4828–4834.
[56] J.F. Nagle, D.A. Wilkinson, Lecithin bilayers—density-measurements and molecular-interactions, Biophys. J. 23 (1978) 159–175.
[57] H. Ebel, P. Grabitz, T. Heimburg, Enthalpy and volume changes in lipid membranes. I. The proportionality of heat and volume changes in the lipid melting transition and its implication for the elastic constants, J. Phys. Chem. B 105 (2001) 7353–7360.
[58] S.L. Veatch, O. Soubias, S.L. Keller, K. Gawrisch, Critical fluctuations in domain-forming lipid mixtures, Proc. Natl Acad. Sci. USA 104 (2007) 17650–17655.
[59] J.A. Killian, Gramicidin and gramicidin lipid interactions, Biochim. Biophys. Acta 1113 (1992) 391–425.
[60] J. Eisenblatter, R. Winter, Pressure effects on the structure and phase behavior of DMPC-gramicidin lipid bilayers: synchrotron SAXS and H-2-NMR spectroscopy study, Biophys. J. 90 (2006) 956–966.
[61] M. Zein, R. Winter, Effect of temperature, pressure and lipid acyl chain length on the structure and phase behaviour of phospholipid-gramicidin bilayers, Phys. Chem. Chem. Phys. 2 (2000) 4545–4551.
[62] M.T. Ge, J.H. Freed, Electron-spin resonance study of aggregation of gramicidin in dipalmitoylphosphatidylcholine bilayers and hydrophobic mismatch, Biophys. J. 76 (1999) 264–280.
[63] T.B. Woolf, B. Roux, Molecular-dynamics simulation of the gramicidin channel in a phospholipid-bilayer, Proc. Natl Acad. Sci. USA 91 (1994) 11631–11635.
[64] B.A. Cornell, L.E. Weir, F. Separovic, The effect of gramicidin-a on phospholipid-bilayers, Eur. Biophys. J. 16 (1988) 113–119.
[65] D. Rice, E. Oldfield, Deuterium nuclear magnetic-resonance studies of the interaction between dimyristoylphosphatidylcholine and gramicidin-a', Biochemistry 18 (1979) 3272–3279.
[66] V.P. Ivanova, I.M. Makarov, T.E. Schaffer, T. Heimburg, Analyzing heat capacity profiles of peptide-containing membranes: cluster formation of gramicidin A, Biophys. J. 84 (2003) 2427–2439.
[67] S. Mitaku, T. Date, Anomalies of nanosecond ultrasonic relaxation in the lipid bilayer transition, Biochim. Biophys. Acta 688 (1982) 411–421.
[68] S. Mitaku, A. Ikegami, A. Sakanishi, Ultrasonic studies of lipid bilayer—phase-transition in synthetic phosphatidylcholine liposomes, Biophys. Chem. 8 (1978) 295–304.
[69] W. Schrader, H. Ebel, P. Grabitz, E. Hanke, T. Heimburg, M. Hoeckel, M. Kahle, F. Wente, U. Kaatze, Compressibility of lipid mixtures studied by calorimetry and ultrasonic velocity measurements, J. Phys. Chem. B 106 (2002) 6581–6586.